Thin Solid Films 680 (2019) 48–54

Contents lists available at ScienceDirect

Thin Solid Films

journal homepage: www.elsevier.com/locate/tsf

The comparison of transient photocurrent spectroscopy measurements of Pulsed Electron Deposited ZnO thin film for air and vacuum ambient conditions

Mehmet Özdoğan[a,b], Serap Yiğen[b], Cem Çelebi[b], Gökhan Utlu[a,*]

[a] Department of Physics, Faculty of Science, Ege University, 35100 Izmir, Turkey
[b] Quantum Device Laboratory, Department of Physics, Izmir Institute of Technology, 35430 Izmir, Turkey

ARTICLE INFO

Keywords:
Photocurrent
Pulsed Electron Deposition
Zinc oxide
Thin film
Atmospheric doping

ABSTRACT

Photoconduction mechanism of ZnO thin films that produced by Pulsed Electron Deposition method is systematically investigated by taking Transient Photocurrent Spectroscopy measurements for different atmospheres including high vacuum and air environments. Response and recovery rates of photocurrent in the air are faster than the rates in high vacuum condition. The results in the presented work clearly indicate that the photoconduction of ZnO thin films with high surface-area-to-volume ratio are surface-related and mostly governed by adsorption/desorption of oxygen and water molecules in the atmosphere. Therefore, the high surface interaction tendency of ZnO surface with the atmosphere inevitably leads to charge transfer from surface to adsorbates and/or vice versa.

1. Introduction

Nanostructured or thin film forms of semiconductors and 2D materials possess an inherently large surface area-to-volume ratio that provides a large active surface area for the interactions of gas molecules. This unique property strongly favors the adsorption of ambient gases onto the surface, and that ultimately leads to sensitive gas detection performance. Materials with large surface area-to-volume ratio can be advantageous for high sensitivity to the surrounding environment (e.g., as a gas sensor [1]), but it could also be problematic for obtaining electrically stable devices (e.g., transistors [2], photodetectors [3], thermistor [4]…etc.), which are expected to operate with low noise levels under atmospheric conditions. The materials with an inherently high surface area-to-volume ratio have been investigated for many years in gas sensors and optoelectronic field [5], but the interactions between surface and atmospheric adsorbates have not been fully understood yet.

Zinc oxide (ZnO) is a promising n-type material for optoelectronic applications due to the wide bandgap of 3.37 eV (at room temp.), and it possesses high free exciton binding energy of 60 meV [6], which make it a potential candidate for UV sensing applications. ZnO is a material studied extensively in the literature, however, it could be also used to study the interactions between surface and atmospheric adsorbates because it has a large surface area-to-volume ratio due to the existing nanoparticles on its surface, which are more likely to occur as a result of high energy deposition techniques such as Pulsed Laser Deposition (PLD) and Pulsed Electron Deposition (PED) [7,8]. Lately, PED method has become a good alternative to PLD, because the PLD has a few drawbacks due to the high costs of laser sources and high safety requirements arisen from the toxic gases. Besides, the PED method maintains the stoichiometry of the target materials in the deposited samples and thus permits the formation of high-quality samples. In the PED method, instead of photons, highly energetic electrons are focused on the target surface in order to ablate material having even large bandgap energy like SiO_2 [9–11]. Although a large number of studies had already been reported in the literature on the structural and physical properties of ZnO thin films, only few studies reported the deposition of the undoped ZnO thin film by PED method [12–14]. Further investigations are still needed to optimize deposition conditions and properties of ZnO thin films for PED method. In addition, ZnO thin film has not been investigated in detail using time-dependent resistivity measurements so far.

In this work, we have systematically investigated to the photo-response characteristics of ZnO thin films for high vacuum and air atmospheres. The PED-produced ZnO thin films have been employed to reveal adsorbate-induced electrical changes in the high surface area-to-volume ratio materials. The results show that the photo-response of the materials with high surface area-to-volume ratio is mainly governed by

* Corresponding author.
E-mail address: gokhan.utlu@ege.edu.tr (G. Utlu).

https://doi.org/10.1016/j.tsf.2019.04.030
Received 6 September 2018; Received in revised form 17 April 2019; Accepted 17 April 2019
Available online 19 April 2019
0040-6090/

the charge transfer process between the ZnO surface and atmospheric adsorbates rather than the expected photo-induced generation and recombination process. Therefore, photoconduction in these materials is largely surface-related rather than bulk-related, and it is highly dependent on atmospheric conditions. The experimentally obtained results are used to interpret the mechanism behind the adsorbate-induced changes in the charge carrier dynamics of other high surface area-to-volume ratio materials.

2. Experimental details

Before starting the deposition of ZnO thin films, the Cr/Au (3 nm/80 nm) interconnect electrodes were patterned on 10 mm × 10 mm fused-quartz substrates by thermal evaporation technique, and the device schematics are given in Fig. 4(c) and (d). In Fig. 4(c), the separation between electrodes was set to 200 μm, and this configuration was used to Transient Photocurrent Spectroscopy (TPS) measurements. In Fig. 4(d), the sample was prepared for van der Pauw measurements. Employing a shadow mask, 130 nm thick ZnO thin films with a size of 4 mm × 4 mm were deposited at the center of quartz substrates by PED method. The details of the PED technique can be found in Ref. [15]. ZnO thin films were deposited by ablating ZnO target (from K.J. Lesker Comp.) with a high purity of 99.999% using the PED system (PEBS-32, Neocera Inc.). The deposition parameters were fine-tuned to achieve the best ablation and plume (i.e., plasma and evaporated material) intensity, and to get high crystal quality of ZnO films. The deposition of ZnO was performed with a substrate temperature of 400 °C, an oxygen pressure of 2.15 Pa, an electron discharge voltage of 15 kV, and a pulse frequency of 5 Hz. The vacuum chamber was evacuated to a base pressure of 1.87×10^{-5} Pa, and a pre-ablation process was applied to get fresh uncontaminated target surface, and then, 1000 successful shots were conducted for ZnO thin film deposition.

After the successful ZnO thin film deposition, we have performed different characterization methods to analyze structural, optical and electrical properties of our samples. Scanning Electron Microscopy (SEM) was performed using Quanta 250 with typically operated at 5.0 kV to analyze the ZnO thin film morphologies. The diameter of the nanoparticles on the surface of the samples were obtained and analyzed by the ImageJ program [16]. The software takes the SEM image of the samples, and it creates a contrast inverted image. The nanoparticles are treated as a circle on this image, but some of the structures don't resemble circular shapes so that by changing the degree of circularity some of these are excluded, and thus, the distribution of the diameter of the nanoparticles is analyzed. In this analysis, the circularity degree is set to 0.60–1.00 (a perfect circle is represented by 1.00) range. The particle diameters were derived from calculated area of each circle using ImageJ software.

The XPS analyses were performed using a Thermo Scientific Model K-Alpha XPS instrument with monochromatic Al Kα radiation (1486.68 eV) under operating pressure set to 2×10^{-7} Pa. Survey spectra and high-resolution spectra were acquired using analyzer pass energies of 30 eV. The X-ray spot size was 300 μm for single point analysis. The number of scans was 10 and dwell time was 50 ms for each data point. All the XPS spectra were calibrated by taking the C 1 s peak located at ~284 eV as a reference. Data were analyzed using Avantage XPS software package. Peak fitting was done using Gaussian/Lorentzian peak shapes and a Shirley/Smart type background.

The X-ray diffraction (XRD) was carried out via a Philips X'Pert Pro Theta/2Theta Diffractometer with a copper K-Alpha X-ray source (λ = 1.540 Å). The scans were performed from 20° to 80° in 0.001° steps. The UV/Vis spectroscopy measurements were made using a Perkin Elmer Lambda 950 UV/Vis/NIR Spectrometer. The scans were performed in 200 nm to 1100 nm range.

The electrical characterizations of the samples were executed using Keithley 2000 Multimeter and Keithley 6220 Precision Current Source. TPS measurements were carried out under the UV irradiation output power of 3 mW (254 nm) in the air and high vacuum environments. For the TPS measurements, a shutter mechanism was coupled to the UV light source, and the photocurrent data of the samples were collected by using Keithley 6485 Picoammeter, and Keithley 2400 Source Meter was used to apply a constant bias voltage of V_b = 1 V. The samples were left overnight under air to return their initial state before each set of measurements, and I-V characteristics of the samples were measured to check whether the samples have the same initial conditions. Afterward, the time-dependent photocurrent measurements were conducted to investigate distinct behaviors of the samples under air and high vacuum conditions. For this measurement, the UV light was switched on for duration of 5 ks, and then switched off for relaxation to another 5 ks. After one day in air, the UV exposure was utilized to remove existing adsorbates from the surface during a period of ~3 h. Right after ~3 h continuous illumination, the TPS measurements were conducted for short periods as 30 s with four on/off cycles.

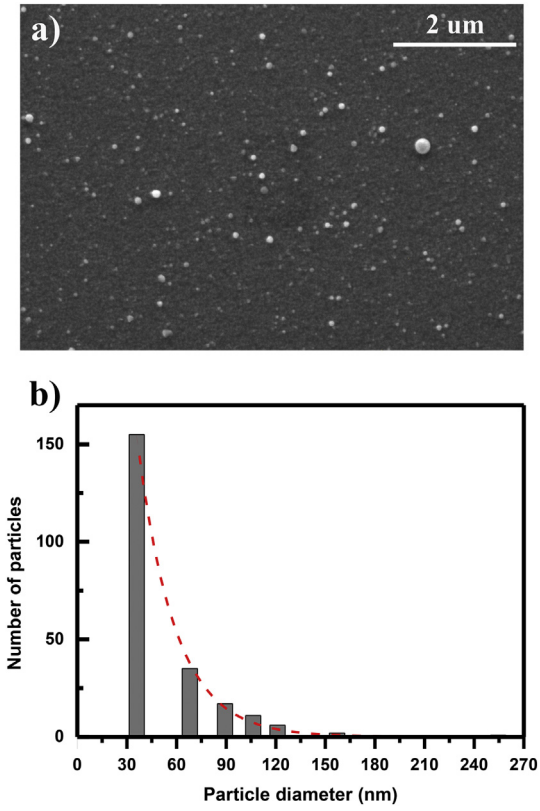

Fig. 1. (a) The surface morphology of the PED-produced ZnO thin film obtained via SEM instrument (typically operated at 5.0 kV). It shows many nanoparticles appearing with as white spots on the surface. (b) The distribution of particle diameter on the PED-produced ZnO thin film surface. Their sizes ranging from ~30 to ~250 nm were observed with a mean particle diameter size of 68.2 ± 3.6 nm. The dashed red curve is a fit by exponential decay function. (For interpretation of the references to color in this figure legend, the reader is referred to the web version of this article.)

3. Results and discussion

The SEM image of the ZnO thin film displays nanoparticles appearing with a lighter color on the film surface as seen in Fig. 1(a). We observed a relatively wide distribution of nanoparticle diameter ranging from ~30 to ~250 nm, with a mean particle diameter of 68.2 ± 3.6 nm as shown in Fig. 1(b). The existence of such particles on the film surface increases the surface area-to-volume ratio, which maximizes the interaction between surface and atmospheric gases, and this consequently leads to unstable electrical device performance. The

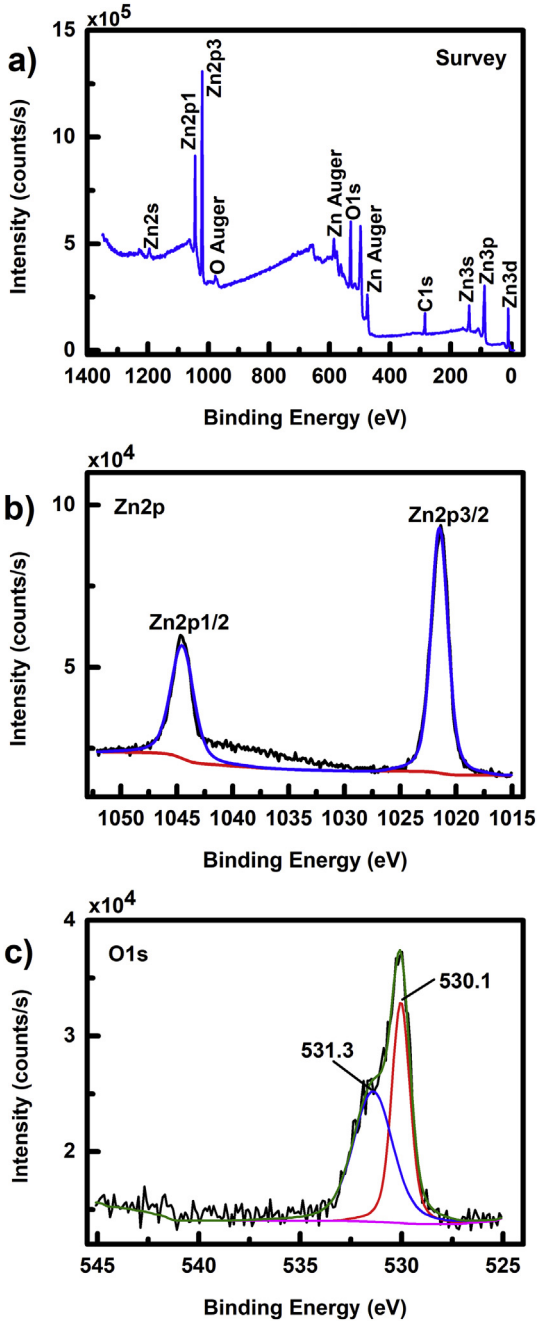

Fig. 2. The XPS spectra of the PED-produced ZnO thin film. A full range survey spectrum was shown in (a), while high-resolution XPS chemical binding spectra of the Zn 2p and O 1 s states (their deconvolutions) were shown in (b) and (c), respectively.

chemical compositions and chemical states of the PED-produced ZnO thin films were investigated by XPS. Fig. 2 (a-c) exhibits survey spectrum and high resolution XPS spectra of Zn 2p and of O 1 s states of ZnO thin film. As seen in Fig. 2 (a), no elements besides Zn, O, and C were detected from XPS survey spectrum. In Fig. 2 (b), the two peaks locating at 1021.3 eV and 1044.7 eV verify that Zn exists in oxidized states [7,17]. Fig. 2 (c) clearly shows the two chemical states of oxygen. The higher binding energy located at 531.3 eV was attributed to the species such as OH, O_2 or H_2O adsorbed on the surface, while lower binding energy at 530.1 was attributed to O^{2-} ions in the hexagonal wurtzite structure of ZnO [18–20]. Therefore this lower peak of the O 1s spectrum could be attributed to the Zn—O bonds, and also, it was associated with O^{2-} ions in the oxygen-deficient regions [21].

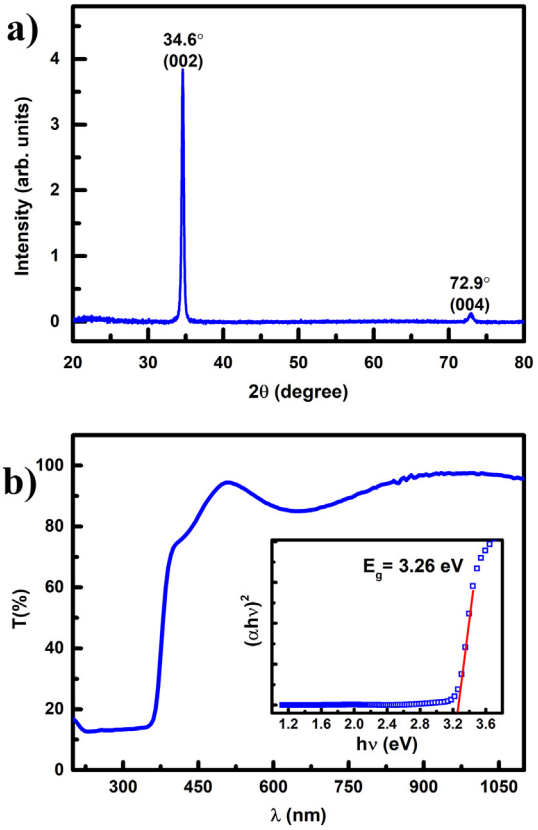

Fig. 3. (a) The XRD pattern of PED-produced ZnO thin film. (b) The optical transmission spectra of the PED-produced ZnO thin film, the inset shows a typical Tauc-plot for the optical bandgap determination.

Fig. 3 (a) exhibits the XRD pattern of PED-produced ZnO thin film. As seen in the XRD graph, the PED-produced ZnO thin films have a single sharp peak around 34.6° and very small peak around 72.9° which were identified as (002) and (004) orientations of hexagonal wurtzite crystal structure, respectively, and highly crystalline phases of the ZnO thin films [6,15]. The highest intensity of plane (002) was attributed to the crystal growth with preferential orientation along c-axis. The crystallite size (D) along (002) plane is 31 nm calculated using the Debye-Scherrer equation ($D = 0.89\lambda/\beta cos\theta$) [22]. The optical transmittance curve of ZnO thin film was presented in Fig. 3(b). It shows high transmittance (> 80%) feature in the visible region with steep fall off at 365 nm, which makes it a potential visible-blind UV photodetector. The inset of Fig. 3 displays $(\alpha h\nu)^2$ as a function photon energy $h\nu$. The extrapolation of the linear part of this curve gives the value of bandgap, E_g. The optical bandgap of ZnO thin films produced by PED method is determined as 3.26 eV. This value is in the same range as those observed in ZnO films obtained by PED or PLD techniques [15,17].

Before each TPS measurements, we conducted I-V measurement for the PED-produced ZnO thin films, and the obtained results were presented in Fig. 4 (a). The initial resistance of ZnO thin film was found to be 35.6 $k\Omega$ before in-vacuum, whereas initial resistance was 30.8 $k\Omega$ before in-air TPS measurement. Therefore, the initial conditions of ZnO thin films for both atmospheres were almost the same before each TPS measurements. In addition, good linear I-V curves of ZnO thin films indicate the ohmic behavior between contacts. However, formation of Schottky contact is expected due to the difference in relative work functions of gold and ZnO [23]. Surface reactivity of ZnO nanostructures induces surface-related defect states within the bandgap, which modify the Schottky barrier with narrowing of its width and/or lowering of its height. For this reason, it is difficult to obtain a Schottky

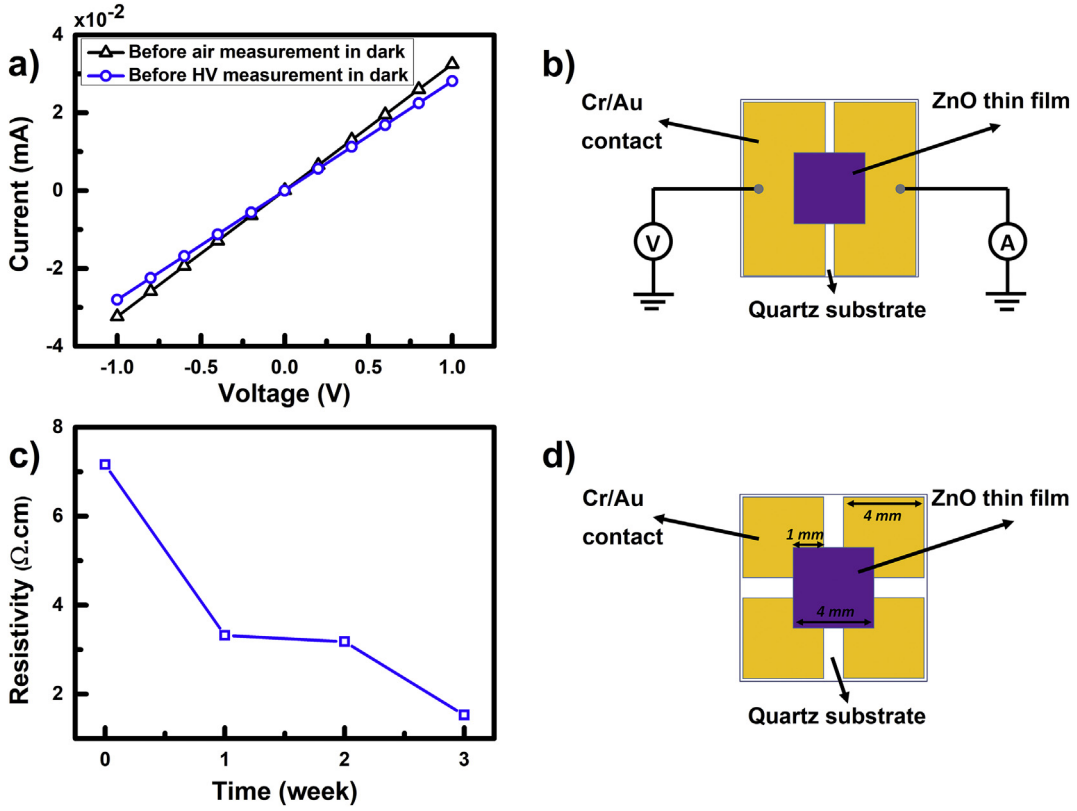

Fig. 4. (a) Dark I-V measurements of the ZnO thin film before vacuum and air TPS measurements. The current data were acquired by sweeping voltage in 0.2 V steps from −1 to 1 V. (b) The device schematic of ZnO-based photoconductor, (c) time-dependent resistivity changes of ZnO thin film, and (d) the van der Pauw configuration for electrical transport measurements of ZnO thin films.

contact for these nanostructures. Also, to check the electrical stability performance of PED-produced ZnO thin films, we carried out time-dependent resistivity measurement weekly using van der Pauw configuration as shown in Fig. 4 (d). The resistivity of our sample decreases gradually as a function of time as seen in Fig. 4 (c). Firstly, the chemisorbed O_2 molecules on the surface increase the resistivity of ZnO thin film since they capture free electrons from the surface. Then, the water molecules are physisorbed on the surface, and they trigger the dissociation of chemisorbed O_2 molecules. Thus, by substitution of oxygen molecules with water molecules, the trapped electrons by oxygen re-introduced the conduction mechanism, and they contributed to current again. This explains why resistivity of our samples decreases in time for our samples. Further, the carrier type and carrier concentration of ZnO thin films as well as their mobility values were determined by conducting Hall Effect measurement on the prepared samples in Van der Pauw geometry. All samples were *n*-type and have a high carrier concentration ($n \approx 10^{19} cm^{-3}$). The measured carrier mobility values were very low, in the order of 1–2 $cm^2V^{-1}s^{-1}$. As known, high carrier concentration results in low mobility value due to the increasing charge carrier scattering [24]. In addition, the adsorbed O_2 molecules on the surface not only reduce the current but also decrease the mobility because of upward band bending [25].

The time-dependent photocurrent measurements were conducted under UV light in high vacuum and air environments applying a constant bias voltage for PED-produced ZnO thin films. Firstly, in order to test high vacuum effect on desorption of adsorbates from the surface, we kept our sample under dark during first 5 ks until reaching the steady state high vacuum condition as indicated in Fig. 5 (a). After 5 ks, the photocurrent decreased only ~1–1.5% according to its initial value as seen in the zoomed plot in the inset of Fig. 5 (a). The physisorption energy of adsorbates to the surface is typically in the range of ~10–100 meV [26–28]. On the other hand, the chemisorption energy of adsorbates is in the order of a few eV [27]. Therefore, we claim that high vacuum just desorbs physically bonded water molecules, and this give rise to very small decrement in the current. When physisorbed water molecules desorbed from the surface, the oxygen molecules near the surface are adsorbed by capturing free electrons near the surface, and these molecules continued to display a decrease in current with respect to time. As a result, high vacuum (5.0×10^{-3} Pa) is not enough to desorb chemisorbed molecules since extra energy is needed to break their chemical bonds like UV light. For this reason, UV light has an energy of ~4.9 eV (254 nm) was chosen since it has sufficient energy for desorbing atmospheric adsorbates from the surface [29] as well as for generating electron-hole pairs in the depletion region of ZnO (E_g ~3.26 eV). Time-dependent current variations of the ZnO samples were given in Fig. 5 (a) and (c). The different behaviors are observed in the current variations for high vacuum and air conditions. First, the photocurrent variation of samples was increased rapidly due to the photogeneration of electron-hole pairs for both atmospheres, and a subsequent slower exponential increase was observed due to the desorption of adsorbates from the surfaces with the help of UV light. The high vacuum assisted to these processes as seen in Fig. 5 (a). In air condition with 40–45% relative humidity (RH), the photocurrent increased very quickly and reached a maximum value (6.5 times larger than its dark value) at ~300 s, and then it gradually decreased until the desorption and re-adsorption of adsorbates reaching to an equilibrium state, where the current was ~4 times larger than its dark value, and it became almost saturated during UV illumination. On the other hand, after a 5 ks period of UV illumination, the variation in current of the ZnO sample was ~45 times higher than its dark value under high vacuum. At the end of 5 ks UV illumination, the increment rate in current variation for high vacuum was ~11 times greater than that of the air. The reason is that under high vacuum, the desorption of adsorbates is more effective than in air, and the desorption/re-adsorption of adsorbates occur

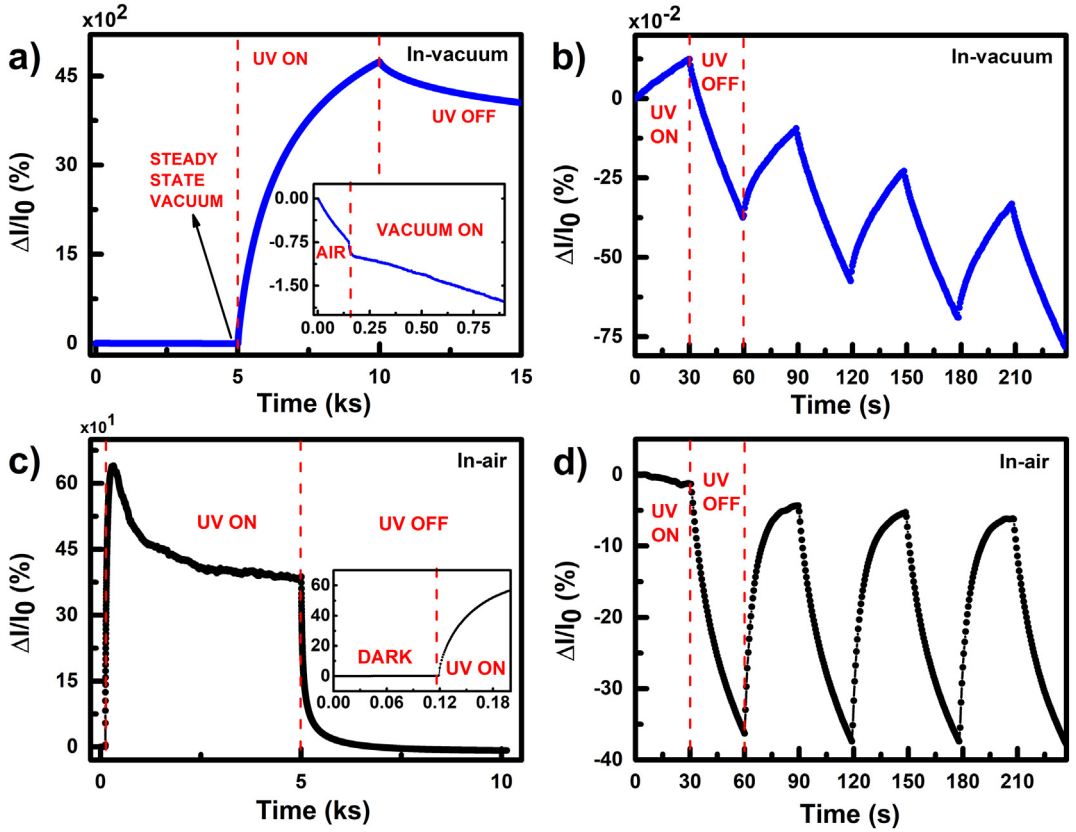

Fig. 5. The time-dependent changes in the current of the PED-produced ZnO thin films which were exposed to 254 nm UV light during a period of 5 ks under (a) high vacuum and (c) air (with 40–45% relative humidity) conditions. After 5 ks, the UV light was turned off, and the samples were let to relax for another 5 ks. The inset of (a) shows the high vacuum effect on current variations, while the inset of (c) shows the dark current read before UV light exposure in air. The short-period TPS measurements of the PED-produced ZnO thin film for (b) high vacuum and (d) air environments. During all measurements, the samples were biased with a constant bias voltage of V_b = 1 V.

during illumination since adsorbate molecules stay too close to the surface in the air. In the event of UV light is turned off, an exponential decay trend was observed for both environments. The adsorbates with lower partial pressure in the middle 10^{-3} Pa vacuum level tend to stick back onto the sample surfaces, however, full recovery of the initial conditions (dark level) of current require longer times > 5 ks, of the order of several hours, because of the adsorbate lacking atmosphere, i.e., high vacuum. The slow recovery of photocurrent is related to the reduced probability of the existence of O_2 and H_2O molecules in a high vacuum. On the other hand, water molecules in air accelerate the decaying of current as they capture more electrons [25,30]. Unlike high vacuum condition, the current decreased the initial value under air when the UV light was turned off as seen in Fig. 5 (c). In the air, the adsorbates stay at the vicinity of the surface, and they are re-adsorbed by the surface more easily giving rise to the quick recovery of current. These results are consistent with previously reported findings in Refs. [25, 31]. Li et al. [25] reported that the effect of oxygen on the photocurrent is more dominant at lower humidity conditions (RH < 60%), whereas the effect of water becomes more significant for higher humidity cases (RH > 60%). Therefore, they experimentally showed that water adsorption, especially at high humidity cases (RH > 70%), leads to the fast shortening of the photocurrent in decaying stage. The reason is water molecules more effectively capture the electrons. The RH in the air was about 40–45% during our measurements that means oxygen had a dominant character on the photoconduction mechanism of our samples. Therefore, a lower oxygen adsorption rate in high vacuum results in a longer electron lifetime and higher photocurrent in comparison to those in the air. Additionally, the observed trend in Fig. 5 (a) agrees with the photocurrent measurements carried out by Lin et al. [31] for oxygen environment.

The TPS measurements were conducted for short periods as 30 s with four on/off cycles to verify the distinct characteristics of the ZnO thin films in high vacuum and air environments, and the obtained results were presented Fig. 5 (b) and (d). Prior to each TPS measurement, the samples were exposed to UV light for duration of ~3 h to remove existing adsorbates in a large amount from their surfaces. Right after ~3 h continuous UV illumination, we started to the short period TPS measurements with setting the shutter on/off period to 30 s. When the illumination was turned on, a very small but sharp increment occurred due to the photo-generation, which is followed by an exponential increase in current due to the photo-assisted desorption process for both environments. With the light was turned off, the photocurrent decreased to its initial level in the air, indicating enhanced stability and reversibility. However, the difference between response and recovery rates caused a downward trend in the overall current variation within a couple of on/off cycles in high vacuum as seen in Fig. 5 (b). In addition, the photocurrent alteration under high vacuum was very small due to the oxygen deficiency; it was < 1%. This small change is related to the low partial pressure of oxygen and water molecules at high vacuum after ~3 h evacuation and illumination process. On the other hand, the alteration of photocurrent in air was > 30% since the oxygen and water molecules stay at the vicinity of surface and play major role on the photoconduction mechanism. Therefore, these molecules can be easily re-adsorbed when the UV light was turned off in the air. These results clearly demonstrate that the photocurrent variations of ZnO thin films are largely due to the adsorption/desorption of adsorbates from the surface rather than fast photo-generation/recombination of electron-hole pairs as in solid state process. In the solid-state process, the photo-

generated electron-hole pairs are expected to occur as rapidly as illumination is turned on. Therefore, response and recovery time of photodetectors must be reached in a couple of μs, even ns [5]. However, the photoconduction of high surface area-to-volume ratio materials like ZnO thin film show a slow response to UV light [32]. The reason is that their high surface area-to-volume ratio increases the interaction with atmospheric gases such as O_2 and H_2O. When they are illuminated with light which has high energy than bandgap, photo-generation occurs but this contribution to current is very small in comparison to the adsorbate-induced contribution to overall current variation. Hence, the small contribution of photo-excited carriers to current is completely suppressed. Also, the adsorbed molecules on the surface create defect states within the bandgap of ZnO, and the photo-excited holes are trapped at these states. The gradual releasing of holes from these defective-states slows recombination rate of electron-hole pairs, which contributes to the slow exponential trend of current [33,34] as seen in Fig. 5 (b) and (d).

ZnO has some challenges such as slow photo-response, electrical stability and stable p-type character problems, which are need to be addressed before possible broad device applications. The slow photo-response under atmospheric conditions has been well known for the photoconduction of the materials with high surface area-to-volume ratio like ZnO thin films [3,30]. In these kinds of materials, the photoconduction process is controlled by adsorption/desorption of some adsorbates such as oxygen and water molecules in the atmosphere. These adsorbates are firstly physisorbed on the surface, and later, they turn into chemisorbed form by capturing electrons. When oxygen is adsorbed on the surface of material, it becomes negatively charged ion by capturing of a free electron from n-type semiconductor, as follows;

$$O_2(g) + e^- \rightarrow O_2^-(ad) \quad (1)$$

and it creates a low conductivity depletion layer in the vicinity of surface. Therefore, the oxygen molecules act as an electron acceptor and significantly change the electrical properties of n-type material since the main charge carriers are captured [25,35]. On the other hand, the effect of water molecule on the photoconduction can be explained by following mechanism;

$$H_2O + 2h^+ + 2e^- \rightarrow H_2 + {}^1/_2O_2 \quad (2)$$

Thus, water can effectively capture the electrons as well as holes. Hence, it more effectively decreases the photocurrent than oxygen when the light is turned off [36]. Eventually, the slow photo-response of the materials having an inherently high surface area-to-volume ratio are strongly dependent on atmospheric conditions [36,37].

The experimental results presented in this work clearly show that the ZnO thin films exhibit different photo-response characteristics under high vacuum and air situations. As known, the oxygen plays a major role in the electrical and optical properties of oxide films. The oxygen vacancies could be found in a large extent in the oxide films, especially the PED-produced films such as ZnO and In_2O_3 [15,38]. The higher content of the oxygen vacancies gives rise to the higher probability of surface defects acting as adsorption sites for the atmospheric molecules. The presented XPS results confirm that these atmospheric molecules such as O_2, H_2O or dissociated water molecules could be easily adsorbed on the surface defects. Additionally, the presented SEM image and particle analysis clearly show that high surface area-to-volume ratio of PED-produced ZnO thin films that makes more sensitive to atmospheric gases. This property of ZnO thin film or other materials with an inherently large surface area-to-volume ratio limit to their broad electronic/optoelectronic device applications. To realize more reliable devices based on the materials with high surface area-to-volume ratio, the surface of these kinds of materials must be properly encapsulated to prevent the effect of environment, and/or a Schottky contact must be formed between contacts to suppress the effects of environment.

4. Conclusion

In conclusion, the photocurrent characteristics of the PED-produced ZnO thin films with high surface area-to-volume ratio were investigated by carrying out TPS measurements for air and high vacuum environments. The adsorbate molecules on the surface are desorbed more effective in high vacuum than in the air under UV illumination. The increment rate in the overall current variation for high vacuum was ~11 times greater than that of in the air at the end of 5 ks UV illumination, and it was not saturated during illumination. When the light was turned off, a persistent current occurred due to the adsorbate-deficient ambient, i.e. high vacuum. However, the photocurrent became saturated as the adsorption/desorption reached to an equilibrium state, and it displayed a reversible switching character in the air. Our results conclude that the photoconductivity of the materials with high surface area-to-volume ratio (e.g, ZnO thin films were presented in this work) is mainly governed by adsorbate molecules in the atmosphere because of their surface interactions. This work clearly indicates that to obtain stable electrical and optical properties for these kinds of material, the encapsulation of the surface is required to get rid of atmospheric effects. Further investigations will be made by encapsulating the surface of PED-produced ZnO thin films, and the obtained results will be shared in another work.

Acknowledgements

The authors would like to thank Center for Materials Research (MAM) of İzmir Institute of Technology, Central Research Test and Analysis Laboratory Application and Research Center (EGE-MATAL) of Ege University and Central Research Laboratories of İzmir Katip Çelebi University for characterizations of samples. This work has been partially supported by the Scientific and Technological Research Council of Turkey (TÜBİTAK) under BİDEB-2232 Program with Project No·117C032 and Ege University Scientific Research Project (BAP) with Project No. 15-FEN-058.

References

[1] F. Schedin, A.K. Geim, S.V. Morozov, E.W. Hill, P. Blake, M.I. Katsnelson, K.S. Novoselov, Detection of individual gas molecules adsorbed on graphene, Nat. Mater. 6 (2007) 652–655, https://doi.org/10.1038/nmat1967.
[2] H. Qiu, L. Pan, Z. Yao, J. Li, Y. Shi, X. Wang, Electrical characterization of back-gated bi-layer MoS 2 field-effect transistors and the effect of ambient on their performances, Appl. Phys. Lett. 100 (2012) 123104, , https://doi.org/10.1063/1.3696045.
[3] S.B. Kalkan, H. Aydın, D. Özkendir, C. Çelebi, The effect of adsorbates on the electrical stability of graphene studied by transient photocurrent spectroscopy, Appl. Phys. Lett. 112 (2018) 013103, , https://doi.org/10.1063/1.5011454.
[4] S.B. Kalkan, S. Yiğen, C. Çelebi, Epitaxial graphene thermistor for cryogenic temperatures, Sensors Actuators A Phys. 280 (2018) 8–13, https://doi.org/10.1016/j.sna.2018.07.028.
[5] K. Liu, M. Sakurai, M. Aono, ZnO-based ultraviolet photodetectors, Sensors 10 (2010) 8604–8634, https://doi.org/10.3390/s100908604.
[6] Ü. Özgür, Y.I. Alivov, C. Liu, A. Teke, M.A. Reshchikov, S. Doğan, V. Avrutin, S.-J. Cho, H. Morkoç, A comprehensive review of ZnO materials and devices, J. Appl. Phys. 98 (2005) 041301, , https://doi.org/10.1063/1.1992666.
[7] A. Ali, R. Henda, R. Fagerberg, Effect of temperature and discharge voltage on the properties of co-doped ZnO thin films deposited by pulsed electron beam ablation, Appl. Surf. Sci. 422 (2017) 1082–1092, https://doi.org/10.1016/j.apsusc.2017.06.123.
[8] M. Nistor, W. Seiler, C. Hebert, E. Matei, J. Perrière, Effects of substrate and ambient gas on epitaxial growth indium oxide thin films, Appl. Surf. Sci. 307 (2014) 455–460, https://doi.org/10.1016/j.apsusc.2014.04.056.
[9] F. Pattini, F. Annoni, F. Bissoli, M. Bronzoni, J.P. Garcia, E. Gilioli, S. Rampino, Comparative study about Al-doped zinc oxide thin films deposited by pulsed electron deposition and radio frequency magnetron sputtering as transparent conductive oxide for Cu(In,Ga)Se 2 -based solar cells, Thin Solid Films 582 (2015) 317–322, https://doi.org/10.1016/j.tsf.2014.11.071.
[10] M. Nistor, N.B. Mandache, J. Perrière, Pulsed electron beam deposition of oxides thin films, J. Phys. D. Appl. Phys. 41 (2008) 165205, , https://doi.org/10.1088/0022-3727/41/16/165205.
[11] P.H. Quang, N.D. Sang, D.Q. Ngoc, Pulsed electron beam deposition of transparent conducting Al-doped ZnO films, Thin Solid Films 520 (2012) 6455–6458, https://doi.org/10.1016/j.tsf.2012.07.027.

[12] M. Nistor, F. Gherendi, N.B. Mandache, C. Hebert, J. Perrière, W. Seiler, Metal-semiconductor transition in epitaxial ZnO thin films, J. Appl. Phys. 106 (2009) 103710, , https://doi.org/10.1063/1.3259412.
[13] D. Calestani, F. Pattini, F. Bissoli, E. Gilioli, M. Villani, A. Zappettini, Solution-free and catalyst-free synthesis of ZnO-based nanostructured TCOs by PED and vapor phase growth techniques, Nanotechnology 23 (2012) 194008, , https://doi.org/10.1088/0957-4484/23/19/194008.
[14] P. Zhan, W. Wang, C. Liu, Y. Hu, Z. Li, Z. Zhang, P. Zhang, B. Wang, X. Cao, Oxygen vacancy–induced ferromagnetism in un-doped ZnO thin films, J. Appl. Phys. 111 (2012) 033501, , https://doi.org/10.1063/1.3679560.
[15] S. Tricot, M. Nistor, E. Millon, C. Boulmer-Leborgne, N.B. Mandache, J. Perrière, W. Seiler, Epitaxial ZnO thin films grown by pulsed electron beam deposition, Surf. Sci. 604 (2010) 2024–2030, https://doi.org/10.1016/j.susc.2010.08.016.
[16] The ImageJ Program, https://imagej.nih.gov/ij/ , Accessed date: 15 April 2019.
[17] M. Naouar, I. Ka, M. Gaidi, H. Alawadhi, B. Bessais, M.A.E. Khakani, Growth, structural and optoelectronic properties tuning of nitrogen-doped ZnO thin films synthesized by means of reactive pulsed laser deposition, Mater. Res. Bull. 57 (2014) 47–51, https://doi.org/10.1016/j.materresbull.2014.05.020.
[18] L.-J. Meng, C.P. Moreira de Sá, M.P. dos Santos, Study of the structural properties of ZnO thin films by x-ray photoelectron spectroscopy, Appl. Surf. Sci. 78 (1994) 57–61, https://doi.org/10.1016/0169-4332(94)90031-0.
[19] Y.F. Lu, H.Q. Ni, Z.H. Mai, Z.M. Ren, The effects of thermal annealing on ZnO thin films grown by pulsed laser deposition, J. Appl. Phys. 88 (2000) 498–502, https://doi.org/10.1063/1.373685.
[20] P.-T. Hsieh, Y.-C. Chen, K.-S. Kao, C.-M. Wang, Luminescence mechanism of ZnO thin film investigated by XPS measurement, Appl. Phys. A Mater. Sci. Process. 90 (2007) 317–321, https://doi.org/10.1007/s00339-007-4275-3.
[21] M. Chen, X. Wang, Y. Yu, Z. Pei, X. Bai, C. Sun, R. Huang, L. Wen, X-ray photoelectron spectroscopy and auger electron spectroscopy studies of Al-doped ZnO films, Appl. Surf. Sci. 158 (2000) 134–140, https://doi.org/10.1016/S0169-4332(99)00601-7.
[22] S.I. Inamdar, K.Y. Rajpure, High-performance metal–semiconductor–metal UV photodetector based on spray deposited ZnO thin films, J. Alloys Compd. 595 (2014) 55–59, https://doi.org/10.1016/j.jallcom.2014.01.147.
[23] Y. Jin, J. Wang, B. Sun, J.C. Blakesley, N.C. Greenham, Solution-processed ultraviolet photodetectors based on colloidal ZnO nanoparticles, Nano Lett. 8 (2008) 1649–1653, https://doi.org/10.1021/nl0803702.
[24] C. Melios, C.E. Giusca, V. Panchal, O. Kazakova, Water on graphene: review of recent progress, 2D Mater. 5 (2018) 022001, , https://doi.org/10.1088/2053-1583/aa9ea9.
[25] Y. Li, F. Della Valle, M. Simonnet, I. Yamada, J.-J. Delaunay, Competitive surface effects of oxygen and water on UV photoresponse of ZnO nanowires, Appl. Phys. Lett. 94 (2009) 023110, , https://doi.org/10.1063/1.3073042.
[26] F.R. Bagsican, A. Winchester, S. Ghosh, X. Zhang, L. Ma, M. Wang, H. Murakami, S. Talapatra, R. Vajtai, P.M. Ajayan, J. Kono, M. Tonouchi, I. Kawayama, Adsorption energy of oxygen molecules on graphene and two-dimensional tungsten disulfide, Sci. Rep. 7 (2017) 1774, , https://doi.org/10.1038/s41598-017-01883-1.
[27] H. Nan, Z. Wang, W. Wang, Z. Liang, Y. Lu, Q. Chen, D. He, P. Tan, F. Miao, X. Wang, J. Wang, Z. Ni, Strong photoluminescence enhancement of MoS 2 through defect engineering and oxygen bonding, ACS Nano 8 (2014) 5738–5745, https://doi.org/10.1021/nn500532f.
[28] S. Tongay, J. Zhou, C. Ataca, J. Liu, J.S. Kang, T.S. Matthews, L. You, J. Li, J.C. Grossman, J. Wu, Broad-range modulation of light emission in two-dimensional semiconductors by molecular physisorption gating, Nano Lett. 13 (2013) 2831–2836, https://doi.org/10.1021/nl4011172.
[29] S.E. Ahn, J.S. Lee, H. Kim, S. Kim, B.H. Kang, K.H. Kim, G.T. Kim, Photoresponse of sol-gel-synthesized ZnO nanorods, Appl. Phys. Lett. 84 (2004) 5022–5024, https://doi.org/10.1063/1.1763633.
[30] Q.H. Li, T. Gao, Y.G. Wang, T.H. Wang, Adsorption and desorption of oxygen probed from ZnO nanowire films by photocurrent measurements, Appl. Phys. Lett. 86 (2005) 123117, , https://doi.org/10.1063/1.1883711.
[31] C.H. Lin, R.S. Chen, Y.K. Lin, S.B. Wang, L.C. Chen, K.H. Chen, M.C. Wen, M.M.C. Chou, L. Chang, Photoconduction properties and anomalous power-dependent quantum efficiency in non-polar ZnO epitaxial films grown by chemical vapor deposition, Appl. Phys. Lett. 110 (2017) 052101, , https://doi.org/10.1063/1.4974924.
[32] C. Soci, A. Zhang, B. Xiang, S.A. Dayeh, D.P.R. Aplin, J. Park, X.Y. Bao, Y.H. Lo, D. Wang, ZnO nanowire UV photodetectors with high internal gain, Nano Lett. 7 (2007) 1003–1009, https://doi.org/10.1021/nl070111x.
[33] J. Jiang, C. Ling, T. Xu, W. Wang, X. Niu, A. Zafar, Z. Yan, X. Wang, Y. You, L. Sun, J. Lu, J. Wang, Z. Ni, Defect engineering for modulating the trap states in 2D photoconductors, Adv. Mater. 30 (2018) 1804332, , https://doi.org/10.1002/adma.201804332.
[34] K. Moazzami, T.E. Murphy, J.D. Phillips, M.C.K. Cheung, A.N. Cartwright, Sub-bandgap photoconductivity in ZnO epilayers and extraction of trap density spectra, Semicond. Sci. Technol. 21 (2006) 717–723, https://doi.org/10.1088/0268-1242/21/6/001.
[35] H.-C. Chang, Y.-J. Huang, H.-Y. Chang, W.-J. Su, Y.-T. Shih, Y.-S. Huang, K.-Y. Lee, Oxygen adsorption effect on nitrogen-doped graphene electrical properties, Appl. Phys. Express 7 (2014) 055101, , https://doi.org/10.7567/APEX.7.055101.
[36] Y. Takahashi, M. Kanamori, A. Kondoh, H. Minoura, Y. Ohya, Photoconductivity of ultrathin zinc oxide films, Jpn. J. Appl. Phys. 33 (1994) 6611, https://doi.org/10.1143/JJAP.33.6611.
[37] J. Zhou, Y. Gu, Y. Hu, W. Mai, P.-H. Yeh, G. Bao, A.K. Sood, D.L. Polla, Z.L. Wang, Gigantic enhancement in response and reset time of ZnO UV nanosensor by utilizing Schottky contact and surface functionalization, Appl. Phys. Lett. 94 (2009) 191103, , https://doi.org/10.1063/1.3133358.
[38] W. Seiler, M. Nistor, C. Hebert, J. Perrière, Epitaxial undoped indium oxide thin films: structural and physical properties, Sol. Energy Mater. Sol. Cells 116 (2013) 34–42, https://doi.org/10.1016/j.solmat.2013.04.002.